OPTIMIZING COMBINED MEMBRANE DEHUMIDIFICATION WITH HEAT EXCHANGERS USING CFD FOR HIGH EFFICIENCY HVAC SYSTEMS

by

Ajay Sekar Chandrasekaran

A Thesis

Submitted to the Faculty of Purdue University

In Partial Fulfillment of the Requirements for the degree of

Master of Science in Mechanical Engineering
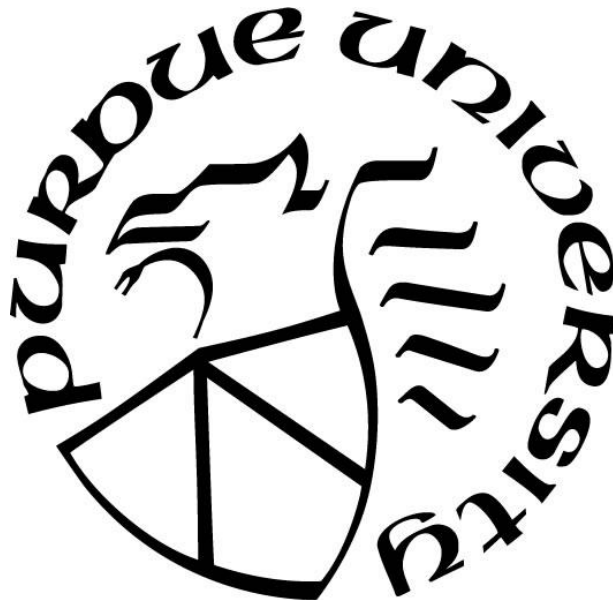
School of Mechanical Engineering

West Lafayette, Indiana

December 2020

THE PURDUE UNIVERSITY GRADUATE SCHOOL
STATEMENT OF COMMITTEE APPROVAL

Dr. David M. Warsinger, Chair

School of Mechanical Engineering

Dr. James E. Braun

School of Mechanical Engineering

Xiulin Ruan

School of Mechanical Engineering

Approved by:

Dr. Nicole L. Key

ACKNOWLEDGMENTS

TABLE OF CONTENTS

LIST OF FIGURES

ABSTRACT

As the energy consumption for thermal comfort and space cooling around the world continues to grow due to a steadily increasing demand and climate change; the use of vapor compression technology, has increased significantly. In this technology, condensation is used to condense out the water vapor from air by maintaining the coils at a cooler temperature than required to meet the sensible load. This results in a high energy consumption for dehumidification and lowers the overall efficiency of the system. They also pose environmental threats due to its significant CO_2 emissions

The aim of this research is to address the above problems by using a novel membrane configuration called as a membrane heat exchanger that has integrated cooling coils and simultaneously cools and dehumidifies the air stream with the help of a vacuum pump and a vapor selective membrane.

In this work, the CFD modeling and design of a membrane heat exchanger is presented. The model is developed for a base case to study the heat and mass transfer performance of the system. The model after validation with existing studies is developed further to obtain several contour plots to understand the effects of concentration polarization, membrane permeance, Reynolds number, pressure drop and other design parameters on the performance of the system.

1. INTRODUCTION

1.1 Global energy crisis

Around 20% of the electricity consumed by buildings is consumed by air conditioning and fans to keep human's comfort. This roughly translates to 10% of global electricity. With increasing migration and climate change, the access to thermal comfort has increased dramatically. Space cooling will account for 35% towards the share of global electricity based on a study by International Energy Agency. The cooling energy is projected to grow at a rate of 5% annually. Most of this energy is contributed by developed countries like United States, Japan where more than 91% of the households already own an AC system. The COP of current air condition systems is 4 on an average depending on the climatic conditions. These facts substantiate the need to reduce the energy consumption of HVAC systems.
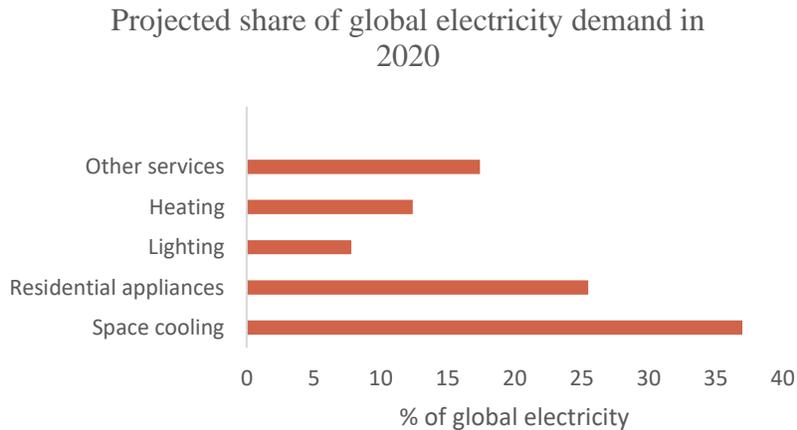
Figure 1: Contribution of different energy consumption applications in buildings
towards the percentage of global electricity
Ref: IEA: The future of cooling [56]
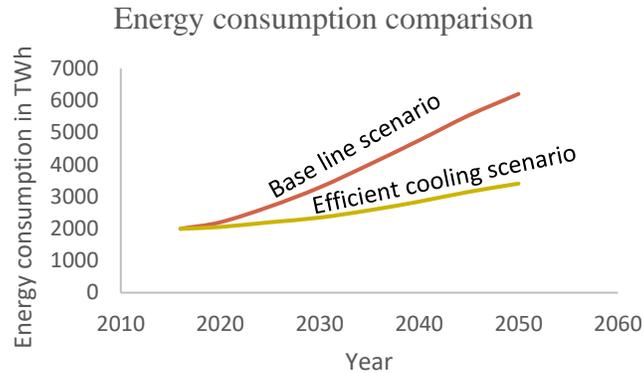
Figure 2: Global electricity share and energy consumption
Ref: IEA: The future of cooling [56]

With baseline scenario which consists of existing HVAC technologies and energy policies, the energy consumption will triple by 2050 which is equivalent to the total combined energy consumed by India and China currently. The efficient cooling scenario consists of using efficient HVAC technologies and improved energy policies. The efficient cooling scenario can help reduce the energy consumption of HVAC technology by 45% by the year 2050.

1.2 Overview of membrane-based system configurations

Membranes have been widely used for different applications from separation of CO_2 in flue gas to dehumidification. Membrane based systems consist of a dense membrane that separates the feed side and the permeate side. Some common examples of membrane-based systems are membrane and condenser, desiccant based dehumidification, two membrane system, membrane energy recovery ventilator [20].

The single membrane system is shown in the figure below. The system consists of a single feed channel in contact with a highly selective porous membrane. This membrane allows only the water vapor to pass through it and not air. The vacuum pump creates the necessary driving force to pull out the water vapor from the incoming air. Since the concentration of water vapor in air is very less, the vapor pressure on feed side is around 1kPa. The vacuum pump pumps out the water vapor

from feed side to the ambient side. This system consumes large amounts of energy due to the high-pressure ratios of vacuum pump.
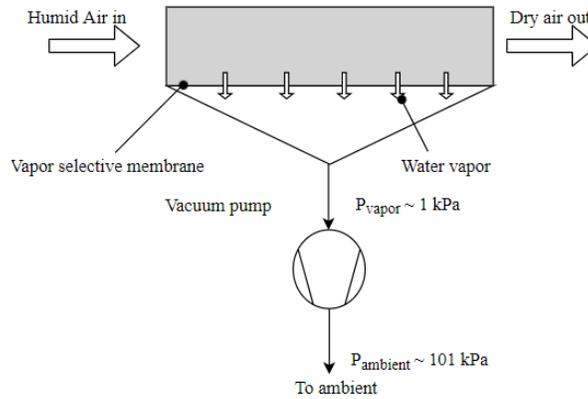
Figure 3: Single membrane system configuration

Vapor selective membrane dehumidifies the incoming air with help of a vacuum pump that pumps the vapor from membrane feed to the ambient

The membrane-based energy recovery ventilator is another common technology used in dehumidification application. The system consists of dense membranes (not selective) that separates the feed and the permeate sides of the membrane. This membrane enables the transfer of both latent and sensible loads between the inlet and exhaust streams of the membrane to and from the building respectively. These systems cannot handle very high latent loads and pollutants can enter the inlet ventilation stream since these membranes are not selective in nature.
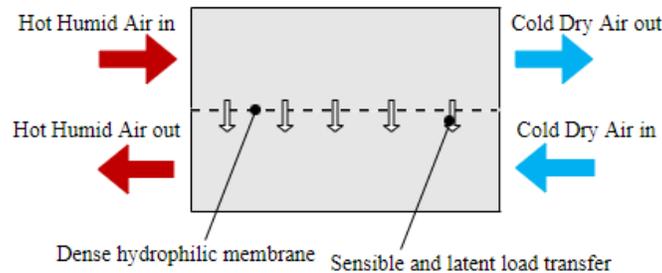
Figure 4: Membrane energy recovery ventilator

Dense membranes help transfer of heat and water vapor between the ventilation and exhaust air streams from the conditioning space

Desiccant based systems are also commonly used in air conditioning applications where a desiccant helps to remove the vapor in air. The desiccants are commonly supported along with a membrane that allows transfer of both latent and sensible loads. The desiccant after absorption of water needs to be regenerated through a heat exchanger so that it could be used again. This process is energy intensive and there is a possibility that the chemicals released from the desiccant can enter into the ventilation air stream.
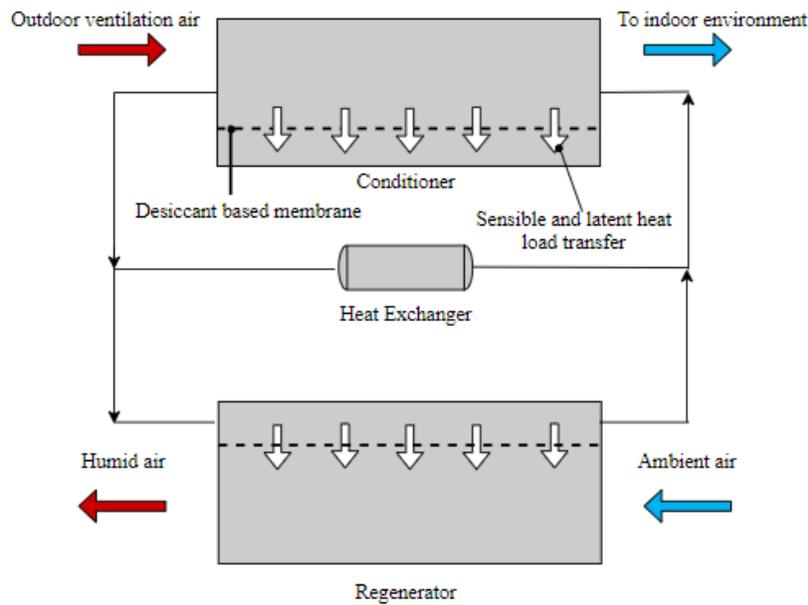
Figure 5: Desiccant membrane-based systems

The desiccant system allows exchange of both sensible and latent loads and needs to be regenerated after absorption of water for using it further

1.3 Thesis statement of objectives

This study aims towards addressing two important challenges in the HVAC industry: to reduce the energy consumption for dehumidification in air conditioning applications worldwide and to reduce the impact of refrigerants in vapor compression system by exploring the use of alternative membrane-based technologies.

While there have been significant advancements in reducing the consumption of energy in air conditioning, most of these improvements have reached their limits and resulted in marginal yields. In vapor compression cycle, the cooling coils are optimized based on the dehumidification load

instead of the sensible load. This introduces two disadvantages: The cooling coils are maintained at a cooler temperature than required to meet the sensile load resulting in high energy consumption of the system and there exists large temperature gradients in the system due to the latent load of condensation reducing the overall COP of the system. This study aims to tackle these problems above by use of novel membrane system that has been developed from previous studies in order to treat the latent and sensible loads independently but simultaneously so that the cooling coils can be optimized only for sensible load performance. This study aims to demonstrate the feasibility of working of a membrane heat exchanger that consists of membrane with intergraded cooling coils through development of CFD model and understand the system performance under a wide range of operating conditions.

2. OPTIMIZING COMBINED MEMBRANE DEHUMIDIFICATION WITH HEAT EXCHANGERS USING CFD FOR HIGH EFFICIENCY HVAC SYSTEMS

Disclaimer: A version of this chapter will be submitted for review and publication in a scientific journal.

2.1 Energy consumption in buildings

U.S commercial buildings consumed about 10% of the total primary energy in 2017 [1]. Of this, HVAC accounts for 30% of total energy consumption [2]. The ventilation air is estimated to constitute about 68% of the latent load in commercial buildings [3]. Energy in buildings has been increasing rapidly due to population growth, migration trends, increased access to comfort control. This signals an increase in the dehumidification load. With this trend expected to rise by an average 5% per year [4] in future with climate change, energy efficiency of buildings has become a major objective of recent energy policies at all levels, be it regional, state or international [5]. Thus, the opportunities for improving the energy efficiency of building services are enormous, and their energy consumption can be cut by more than 30%, on average, by using more efficient technologies than those available on the market today [6].

2.2 Overview of current HVAC technologies

Traditionally, latent and sensible loads have been treated in a coupled manner such that the cooling coils temperature is set based on dehumidification load. Thus, the coils are maintained at a cooler temperature than required to meet the sensible loads. This also leads to large temperature gradients and large condensation heat loads associated with condensation dehumidification. In order to meet the CO_2 emission goals commitment set by US Department of Energy [7], alternatives to vapor compression technology are required. Many research studies have focused on improving the configuration, materials and heat transfer performance of heat exchangers that have made progress but has approached maturation or diminishing returns [8-12]. A study by the US Department of Energy showed the energy savings potential of using membrane-based systems as 2.3 Quads/year [13,14]. Thus, this study focuses on studying the performance of a novel configuration of

membrane heat exchanger using a selective membrane-based system that simultaneously cools and dehumidifies the air with help of a vacuum pump.

2.2.1 Membrane based dehumidification technologies

Membranes have been used for different applications such as desalination [15-16], CO_2 separation from flue gas and dehumidification. A common air conditioning application is the membrane-based energy recovery ventilator [17 – 19]. These devices transfer both sensible and latent energy between incoming and exhaust air streams leaving an indoor space that are separated by membranes. They are essentially heat exchangers that can also exchange vapor by diffusion Due to their lower membrane selectivity, they can only provide partial dehumidification and can allow pollutants in from the other air stream[20,21]. Another common membrane technology is the liquid based desiccant air conditioning which removes water vapor from the air with a liquid desiccant membrane-based system. These systems require energy intensive desiccant regeneration processes and there is a risk that the desiccant may contaminate the ventilation air stream causing duct damage and affecting the indoor air quality [22,23]. Additionally, in highly humid cities like Houston, these technologies result in a higher energy consumption [24] compared to air conditioners without active humidity control. Vapor selective membrane-based technologies helps overcomes these challenges by treating the latent and sensible loads independently with the help of highly selective membranes so that the cooling coils can be optimized to meet only the sensible load requirements.

2.2.2 Selective membrane-based dehumidification

Vapor selective membrane-based dehumidification systems use a vacuum pump to mechanically separate the water vapor from an air stream. Compared to removing water vapor from air through condensation, the removal of water vapor using selective membranes and vacuum pump is more energy efficient as the heat transfer performance of cooling coils can be optimized with respect to only the sensible load. This also helps avoiding large energy penalties associated with condensation of water vapor from air. This ensures that the sensile cooling can be provided efficiently at higher cooling temperatures and enables a better control of latent loads. A study by Labban et al. (2017) shows the potential of several different membrane-based solutions, as well as

the performance of desiccant systems and conventional vapor compression systems. The study concluded that membrane-based cooling systems can have a COP two times higher than the current vapor compression cooling systems. The most promising membrane technology was the one which employed two vapor selective membrane modules [25]. This approach enables smaller pressure ratios across the vacuum pump, thus greatly reducing the energy input required, compared to membrane dehumidification systems which reject the water vapor straight to atmospheric pressure [26,27]. The designs here improve upon that approach.

2.2.3 Overview of CFD modelling for membrane applications

Most previous works have focused on using CFD to study the gaseous separation process of CO_2 or hydrogen species using membranes [14,23,24,28] or to study the effect of spacers on the system performance [29]. Bui et al (2015) [30] studied the isothermal dehumidification process of a membrane using CFD to understand the tradeoff between membrane dehumidification and its COP. CFD models have been used widely to study the effect of spacers and concentration polarization on heat and mass transfer performance of membrane and also for membrane dimension optimization. In this study, we focus on the heat and mass transfer properties of a membrane module that employs vapor selective membranes for dehumidification and cooling channels built into the module to provide simultaneous sensible cooling. No such membrane system, that incorporates simultaneous cooling, has been studied from a CFD perspective The CFD model presented herein can be used to understand important tradeoffs between the different performance metrics of the system [31].

2.2.4 Literature Summary

A summary of important points from the literatures discussed so far is presented here.
- The use of condensation to remove the vapor from air is energy intensive and inefficient from an overall efficiency point of view.
- Membrane based technologies have the scope to reduce the energy consumption in air conditioning industries and have a COP of 2-4 times the COP of existing systems.
- CFD has been widely used in membrane technologies for studying effects of spacer configurations on the membrane performance.

- Studies have shown that circular cooling coils combined with cross flow configuration is efficient compared to other configurations.
- Flat plate membrane configurations have been widely used for membranes due to their high efficiency

2.3   System description

The membrane heat exchanger shown in figure 2 is a non-isothermal system which uses a vapor selective membrane to dehumidify the incoming air stream while simultaneously cooling the air. The selective membrane ensures that only water vapor passes through the membrane. This facilitates the integration of membrane and sensible cooling within a single module [32,-34]
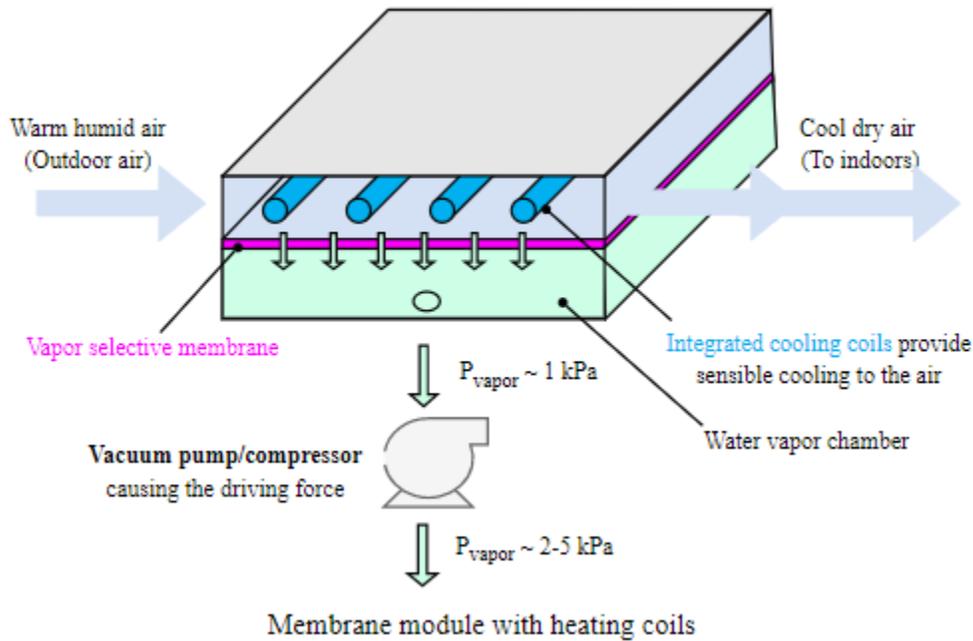

Figure 6 Membrane heat exchanger design.

This design simultaneously cools the warm humid air while dehumidifying it with the membrane helping to avoid high energy associated with the condensation of water vapor and a better control over humidity

Warm and humid air from outside enters the feed side of a membrane module (fig 1 left). A vacuum pump or compressor pulls out the vapor from incoming air through the vapor selective membrane (fig 1 bottom). Ideally, this membrane will allow only water vapor transport, and not air, but in reality, the membrane would allow a small amount of air to pass through. With the vacuum pump creating a suction pressure on the permeate side of membrane module, the vapor pulled by the pump is transferred to the feed side of another exhaust membrane module [35,36] (fig 1 bottom) that is not shown here for brevity. The membrane module also cools the incoming fluid stream simultaneously through the cooling coils which are maintained at a cold temperature through vapor compression cooling system. Since the incoming humid air is already dehumidified, cooling the air does not cause any condensation within the system (fig 1 right).

2.4   Modelling Methodology

A 2D CFD model was developed using STAR CCM+ to study the dehumidification performance and concentration polarization effects of the membrane heat exchangers, heat transfer of air stream to be dehumidified. User defined equations are specified to define the mass transfer performance of membrane. The membrane is modelled as a thin permeable wall between the feed and permeate sides of the intake membrane module. The CFD results from the model (the temperature drop, condensation, heat transfer coefficient) are validated with an analytical model and then used for parametrization. The following assumptions have been considered while developing the CFD model

1. Humid air is considered to be an ideal gas mixture consisting of only two components - water vapor and dry air
2. The fluid flow through the channel is considered to be steady and incompressible
3. The physical properties of the humid air are based on mixing law
4. The effect of temperature on the physical properties of the humid air mixture is considered to be negligible
5. Both air and water vapor permeate through the membrane independently.
6. The cooling coils are always maintained at a constant temperature
7. The vacuum pump always maintains a constant operating pressure across either side of the membrane

17

8. The fluid film formed on cooling coils during condensation (if any) offers a minimal resistance to the heat transfer occurring between the cooling coils and fluid stream in the channel.

9. The fluid film formed from condensation (if any) on the cooling coils remains stagnant and the effect of gravity on the film is neglected

2.4.1 MHX channel configuration

Long thin membrane channels are the most widely used due to their superior performance and their ease of manufacture. The design uses a flat plate channel with integrated cooling channels in an inline arrangement. In addition, small narrow channels have a higher mass transfer effectiveness due to the small diffusivity of water vapor in air. This design also uses an in-line tube arrangement that facilitates a continuous temperature drop as the air flows across the channel. The minimum diameter of cooling coils is constrained by the minimum size commercially available in the current market. Circular cooling channels in total heat exchangers perform well compared to other cooling channel configurations [22]. For simplicity, in the current system, the fluid in cooling coil is not modelled explicitly. The baseline dimensions of the system are chosen to reasonably compare with lab-scale membrane-based process prototypes like membrane distillation and membrane-based energy recovery ventilators [37-39]. Figure 3 below shows the CFD model used in current study along with initial base dimensions.
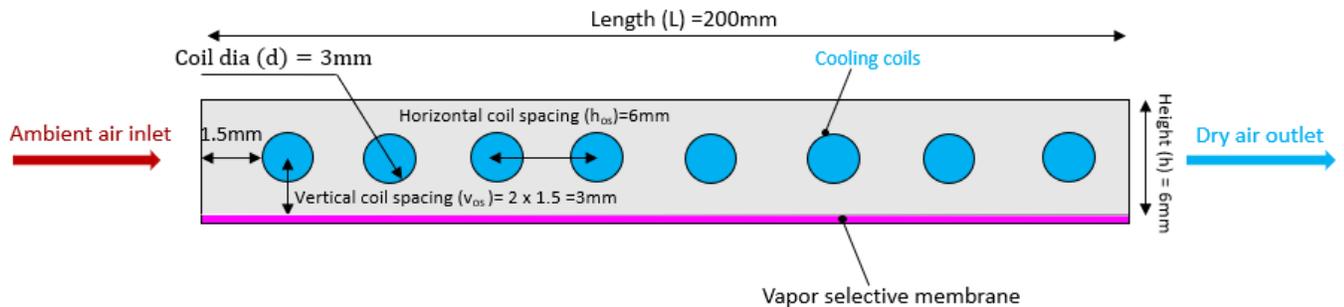

Figure 7: Baseline 2D CFD model for the study with initial base dimensions and their corresponding notations.

Baseline dimensions are used to initially study membrane heat exchanger performance and are optimized further from CFD parametric sweep results

2.5   Governing equations

2.5.1   Mass and momentum equations

The mass, momentum, energy, species transport and condensation equations available in CFD are used while the mass transfer across the membrane is specified with user defined equation. The mass conservation equation is based is written as

$$\nabla.(\rho_i \vec{v}) = S_{m,i} \tag{1}$$

where ρ_i is the density of each species i and $\vec{v}$ is the velocity vector. $S_{m,i}$ is the source of mass of each species due to phase change, ∇ is the standard derivative of given quantity. The mass conservation equation is solved for each species within the system. This equation is used to conserve the mass of vapor and air within the system. The momentum conservation equation is given by

$$\nabla.(\rho \vec{v}) = -\nabla p + \nabla \overline{\overline{\tau}} \tag{2}$$

where ρ is the density of fluid mixture, ∇p is the pressure gradient responsible for the fluid flow in the system and $\overline{\overline{\tau}}$ is the stress tensor due to viscous term. The negative sign indicates that the fluid flows from a high-pressure region to a low-pressure region. A single momentum equation is solved for all species present within the system and solves for the velocity of air and pressure drop in the channel.

2.5.2   Energy equation

A single energy equation is solved for all species in the system and gives the temperature field. The energy conservation equation is.

$$\nabla.(\rho \vec{v} c_P T) = \nabla k \Delta T + m_i h_{fg} \tag{3}$$

where c_p is the specific heat of the fluid mixture, k is the thermal conductivity of the fluid mixture, ΔT is the temperature gradient in the system, m_i is the rate of condensation and h_{fg} is the latent

heat load of condensation. The energy equation is used to solve for heat transfer performance in the system.

2.5.3 Species transport equation

The species transport equation solves for concentrations of air and vapor species in the system. The equation is given by

$$\nabla.\,(\rho\vec{v}Y_i) = -\nabla.\,\rho D_i,\nabla Y_i \tag{4}$$

where Y_i and D_i are the mass fraction and diffusivity of each species (water vapor and air) within the system.

2.5.4 Mass transport through membrane

The mass transport across the membrane interface is governed by a user-defined function based on Fick's law of diffusion [40] described as

$$J/A = B*(P_{vf} - P_{vp}) \tag{5}$$

where J/A represents the mass flux across the membrane interface, with J being the mass flow rate of each species through the membrane and A being the area of the membrane. B is the permeance of membrane, which is a measure of how well each species passes through the membrane. P_{vf} and P_{vp} are the partial pressure of each species on feed and permeate sides of the membrane interfaces respectively. Although, the mass transport equation across the membrane is a function of membrane properties like pore diameter, tortuosity, and porosity, a simple linear expression as a function of only vapor pressures and permeability has been used as a standard assumption.

2.5.5 Condensation mass transfer

The condensation model is used to understand the rate of unwanted condensation by the cooling coils in the system. After optimizing the system dimensions to prevent condensation, the absence of condensation within the system can be verified by ensuring that the maximum value of relative

humidity in the system does not exceed 1. The condensation rate was determined according to Equation 6 [41]

$$\dot{m}_1 = k * A_{coils} * \rho_{H_2O} * (Y_{H_2O,\infty} - Y_{H_2O,w})$$ (6)

where $\dot{m}_1$ is the condensation rate, k is the mass transfer coefficient determined from the Schmidt number, A_{coils} is the cooling coil surface area, ρ_{H_2O} is the density of water vapor and $Y_{H_2O,\infty}$ and $Y_{H_2O,w}$ are the mass fraction of vapor in the bulk air and on cooling coil walls respectively. The equation is activated when the vapor concentration at the wall interface reaches saturation conditions.

2.5.6 Mesh independence study

A mesh independence study was conducted to ascertain that the CFD results do not depend on the mesh size. This study shows a mesh size of 0.007m as the optimal size. The grid study meshes the region around the cooling coils using a meshing method called prism layer meshing to ensure a smooth mesh transition. The meshing also uses the wake mesh setting within STAR CCM+ to prevent the formation of recirculation at the channel downstream. The mesh independence study plot is given in the supplemental section.

2.5.7 Boundary and Operating conditions

A dry air and water vapor mixture enters the feed channel at 27^OC and a vapor mass fraction of 0.025 (RH:70%) at the inlet. These conditions are chosen to represent a warm humid climate. The cooling coils was maintained at a constant temperature of 10^oC. The pressure in the channel feed and permeate sides are 101.325 kPa and 1 kPa [42,43] respectively. The removal of air and vapor across the feed and permeate sides of the membrane is specified using (6). The membrane permeance in this study has a median value of 5000 GPU which matches different studies [44-51] and is assumed to have a high selectivity to water vapor (i.e. very little air passes through) [52-53]. Hence, the vapor and air mass fractions on the membrane permeate side are set as 0.99 and 0.01 for the initial conditions.
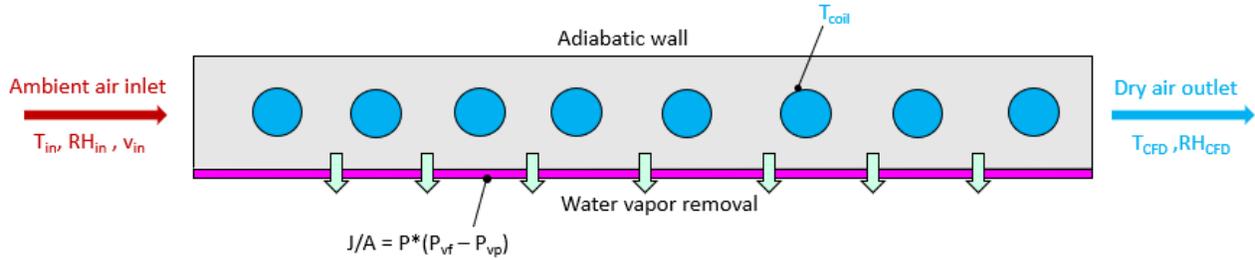
Figure 8: Boundary conditions used for CFD with initial base dimensions.

The inlet boundary conditions are chosen to mimic a warm humid climate and a typical HVAC operating conditions at the outlet. Inlet boundary condition is maintained at 27OC,70% RH for most cases

2.5.8 Analytical validation

Validation and verification of CFD model is an important step towards ensuring that the model developed is accurate and reliable. The temperature, pressure drop, heat transfer coefficient and rate of condensation from CFD model was validated with an analytical model of an external flow over a tube bank [54,55]. The mass transfer trends from CFD match well with the results of CFD modelling of direct contact membrane distillation system [40]. The temperature drop across the tube bank is calculated using the equation (S2) in a supplemental section. Figure 7 shows the temperature drop comparison between CFD and the analytical models with a 2% error. This error is due to the difference in geometry and flow type for the CFD and analytical model. In the CFD model, the fluid flow is restricted by the walls of channel. This increases the fluid's velocity between the coil and channel wall. This explains the quicker temperature drop from CFD compared to the analytical study. The average heat transfer coefficients from the analytical and CFD studies are 56 W/m^{2}K and 60 W/m^{2}K respectively with an error of 7%. The pressure drops from the analytical model calculated using equation (S3) in supplemental and CFD are 27.8Pa and 29Pa respectively with an error of 4.3%. The condensation rate from the analytical model using equation (S4) in supplemental and CFD model are 0.015kg/s and 0.0147 kg/s respectively with an error of 2%. The method of calculation of these variables from the analytical model are described in the supplemental document.
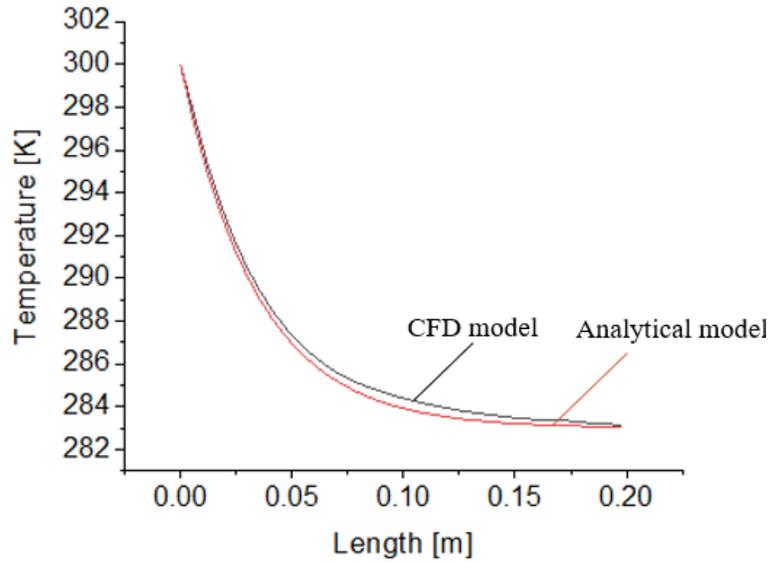
Figure 9: Validation of CFD model with analytical model modelling cooling of air by coils perpendicular to the flow direction

The graph shows the temperature drop along channel length matches well between the analytical and CFD models.

2.6   Results and Discussions

The initial base model was developed further to obtain 50 data points for each of the contour plots between different design parameters of the membrane heat exchanger

2.6.1   Performance study of membrane heat exchanger: CFD contour plots

CFD contour plots of the temperature, relative humidity and specific humidity are shown in figure6.
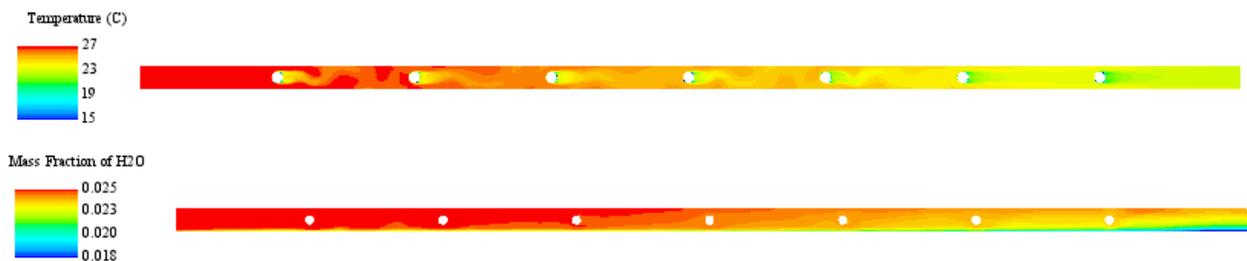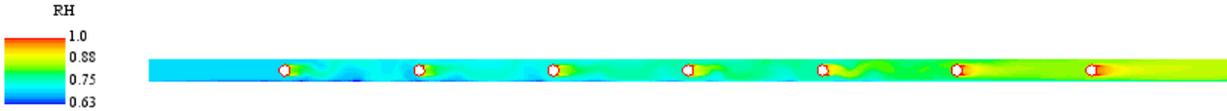
Figure 10: CFD contour results for temperature, specific humidity and RH.

L x W x H= 0.6 m x 0.006 m x 1 m v_{in}=5m/s,T_{in}=27°C, RH_{in}=70%, T_{coil}=10°C, B=3500 GPU. Turbulent flow (Re = 4500) improves heat and mass transfer performance

2.6.2 Effect of channel height and coil diameter on heat transfer performance

The optimal channel dimensions for tradeoff and its impact on the heat transfer are presented here. The variation between the channel height and coil diameter and its effect on the temperature drop of the air is presented here in Figure 6. Temperature drop of the fluid after the first cooling coil decreases with increasing the channel height for a given coil diameter due to the temperature boundary layer effects leading to a smaller temperature drop. Smaller channel heights also help to enhance the mass transfer of the system due to a higher Schmidt number. Additionally, larger diameter coils with smaller channel heights result in high pressure drops. However, smaller coil diameter also has a negative impact on heat transfer. Thus, there exists a tradeoff between the coil diameter and channel height and d/h ratio should be chosen depending on outlet temperature to be achieved.
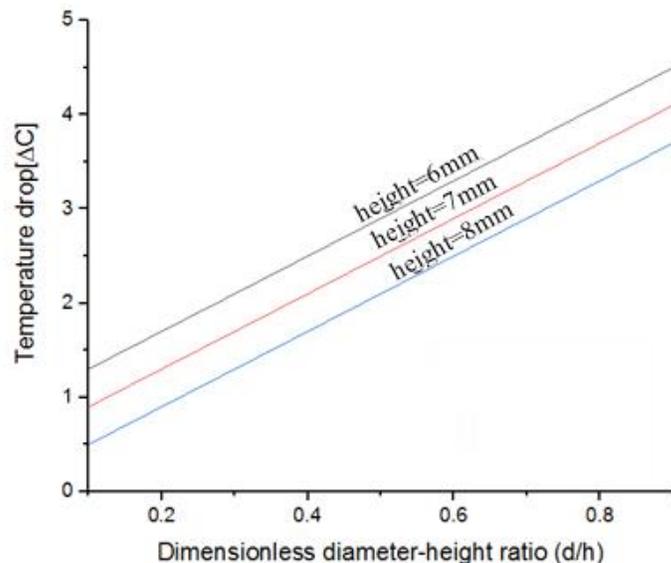
**Figure 11: Temperature drop variation with d/h ratio.**

T_{in}=27°C, RH_{in}=70% ,v_{in}=1m/s, N_{coils}=33 coils, T_{coil}=10°C ,L =0.2 m, H =0.006m, v_{os}=h_{os}=0.006m, B=5000 GPU. Coil diameter varies for a given channel height.

2.6.3 Effect of channel height and coil diameter on the pressure drop

The effect of diameter to channel height ratio and Reynolds number on pressure drop is depicted in figure 9. The pressure drop in the channel increases with increasing coil diameter to channel height ratio (d/h) and does not depend on the Reynolds number for a given d/h ratio. Increasing the coil diameter for a given channel height decreases the area between coil and channel wall resulting in higher velocities. Since higher velocities correspond to higher pressure drop, pressure drop also increases.   When the d/h ratio is increased from 0.1 to 0.35, there is no significant pressure drop increase compared to the pressure drop increase by 250% from 100Pa to 350Pa when increasing d/h ratio from 0.4 to 0.9. The d/h ratio depends on the target temperature to be achieved at channel outlet. Hence for any given Reynold's number, it is advisable to maintain diameter of coil to channel ratio in the range of 0.1-0.35 for a given channel height with current operating conditions in order to avoid increases in the pressure drop which would increase the fan work.
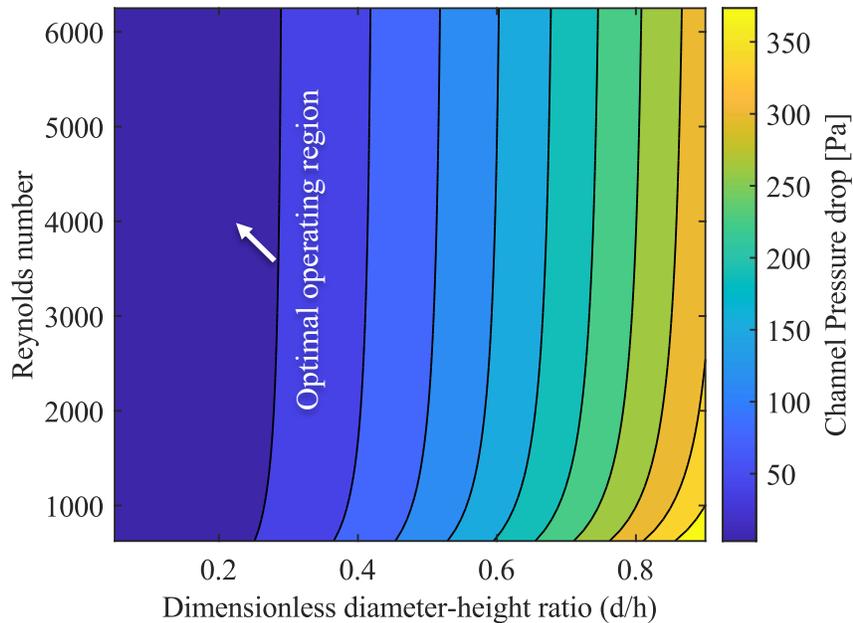
Figure 12: Pressure drop minimization

T_{in} =27°C, RH_{in}=70%, T_{coil} = 10°C,L x H x W = 0.8m x 0.006m x 0.3m,N_{coils}=8,v_{os}=0.006m,h_{os}=0.08m, B = 5000GPU.There are not substantial changes with Re once the flow is turbulent (Re>2300) but larger diameters cause substantial pressure penalties.

2.6.4 Impact of channel length and horizontal coil spacing on heat transfer

The optimal channel length and horizontal coil spacing for tradeoff and its impact on the heat transfer are presented here and are shown in Fig 9. At smaller horizontal coil spacings, there occurs secondary flows in the channel due to under developed flow resulting in smaller temperature drops (fig 9 left). When the horizontal coil spacing is increased beyond a certain threshold, the fluid is fully developed and thus the temperature drop remains constant (fig 9 right). The horizontal coil spacing also depends on other factors like coil diameter, Reynolds number, the channel height and the membrane area to avoid condensation. For the current study, the ratio of horizontal coil spacing to channel length for which flow becomes fully developed in the channel is 0.025.
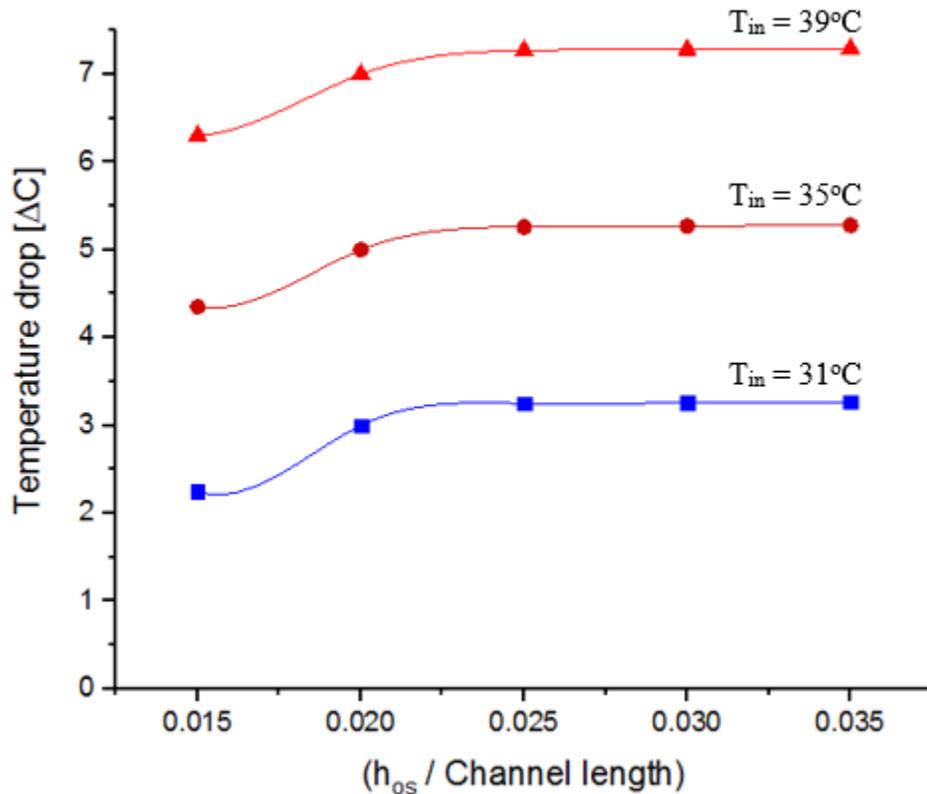
Figure 13: Channel length effect on heat transfer.

T_{in}= 27°C, RH_{in}=70%, v_{in}= 1m/s, T_{coil}=10°C, H=0.006 m, diameter$_{coolingcoils}$= 0.003m, v_{os}=0.006m, B=5000GPU. Horizontal coil spacing is varied to obtain 33 cooling coils in the channel equidistant from each other.

2.6.5 Tradeoff between channel length and Reynolds number on membrane area

The most important tradeoffs for high performing systems revolve around membrane area. Comparing this with Reynolds number and channel length (Figure 10) is the broadest way to see these key design tradeoffs. The optimal channel length for which the total membrane area is minimized is identified as 0.6m for the current scenario. At smaller channel length and larger channel depth, the mass flow rate of air through the channel is more compared to the mass flux of vapor pulled out by the membrane resulting in a very large membrane area especially at laminar regime (Re<2000) (left bottom). Increasing Reynolds number from laminar to turbulent regime decreases the membrane area required. For example, given a channel length of 0.3m, increasing the Reynolds number from 1000 to 4000 decreases the membrane area required by 50%. Increasing the Reynolds number beyond turbulence regime yields minimal benefits (left top). As the channel length is increased, the amount of vapor pulled by the membrane becomes comparable with the channel air mass flux resulting in smaller membrane areas (right bottom). Increasing this channel length beyond a threshold value does not yield any benefits. For example, increasing the channel length from 0.2 to 0.6m decreases the membrane area by 68% while increasing the channel length above 0.6m does not yield benefits. Thus, the optimal channel length which minimizes membrane area must be chosen based on latent load requirements and membrane permeance. The channel length must also be sufficient to fit all the cooling coils to meet the required target temperature at the channel outlet.
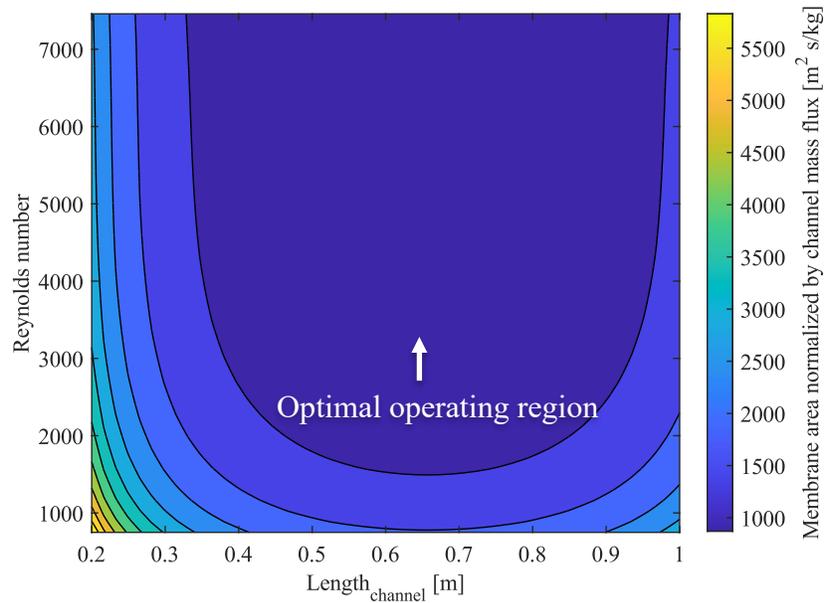
Figure 14: Membrane surface area minimization

T_{in}=27°C, RH_{in}=70%, T_{coil}=10°C, H = 0.006 m, N_{coils}=8, $diameter_{cooling\ coils}$= 0.003 m, v_{os}= 0.006m. B=5000GPU while the horizontal coil spacing is varied to accommodate 8 coils depending on the channel length. W is varied to produce J/A =0.00005 kg/s.

2.6.6   Membrane permeance Vs membrane area tradeoff

The membrane area tradeoff with membrane permeance and humidity load is presented here. The membrane area required for a given humidity load is not significantly limited by the membrane permeance beyond a certain value and depends strongly on amount of amount humidity reduction to be achieved (figure 10). For smaller amounts of humidity reduction around 0.001-0.0015 kg moisture/kg dry air, there is negligible reduction in membrane area obtained by increasing membrane permeance from 2000 GPU to 10000 GPU. At high humidity reductions around 0.002-0.035, increasing the permeance from 2000 GPU to 6000 GPU decreases the membrane area by average of 65%. Increasing the membrane permeance further does not result in significant membrane area reductions. Hence, a membrane permeance around 5000-6000 GPU seems feasible enough for a system to be operated in real time conditions and also avoid significant effects of concentration polarization.
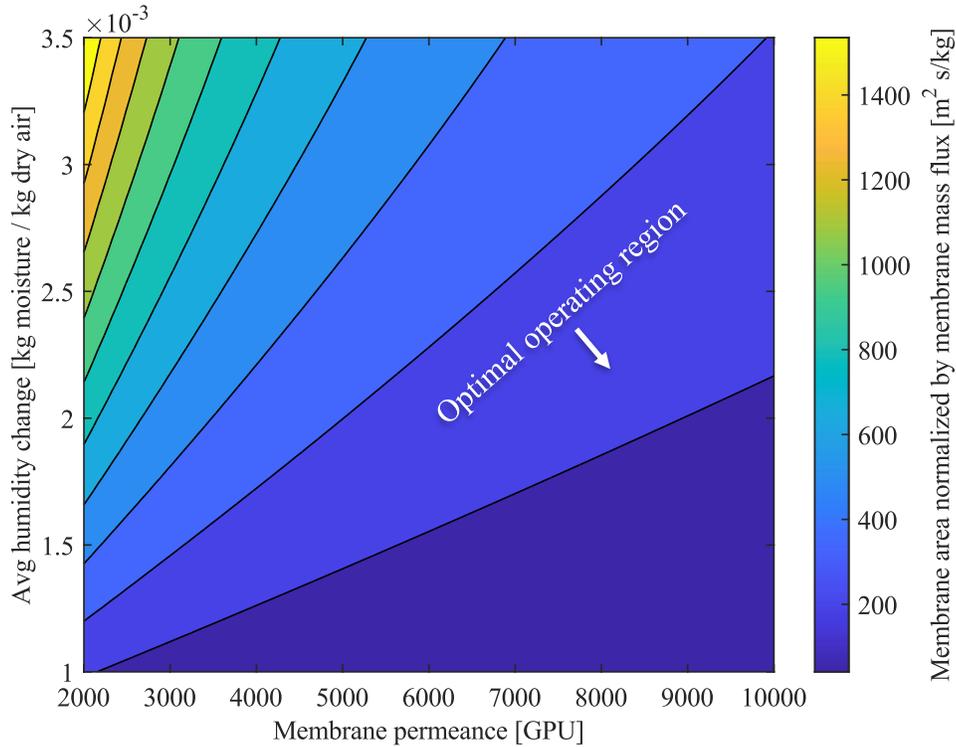
Figure 15: Impact of membrane permeance on humidity load to minimize normalized membrane area.

$T_{in}=27^{\circ}C$,$T_{coil}=10^{\circ}C$,H=0.006 m, $N_{coils}=8$,$v_{os}=0.006$m and $h_{os}=0.08$ m. Increasing permeance yields diminishing returns especially with reduced dehumidification needs (bottom right region)

2.6.7 Concentration polarization dependence on Reynolds number and Membrane Permeance

Concentration Polarization is an important performance characteristic that affects the mass transfer of membrane-based systems. Comparing this with the Reynolds number and membrane permeance (fig 12) can help optimize the membrane mass transfer effectiveness. At smaller Reynolds number and membrane permeance, there is very little concentration polarization (bottom left region). Increasing the Reynolds number increases mixing within the channel decreasing the effect of concentration polarization. Higher membrane permeance leads to a higher concentration polarization as the membrane causes a greater deficiency of vapor at the membrane surface (bottom right region). Membrane permeance in the range of 4000-6000 GPU seem to be the optimal value to avoid effects of concentration polarization.
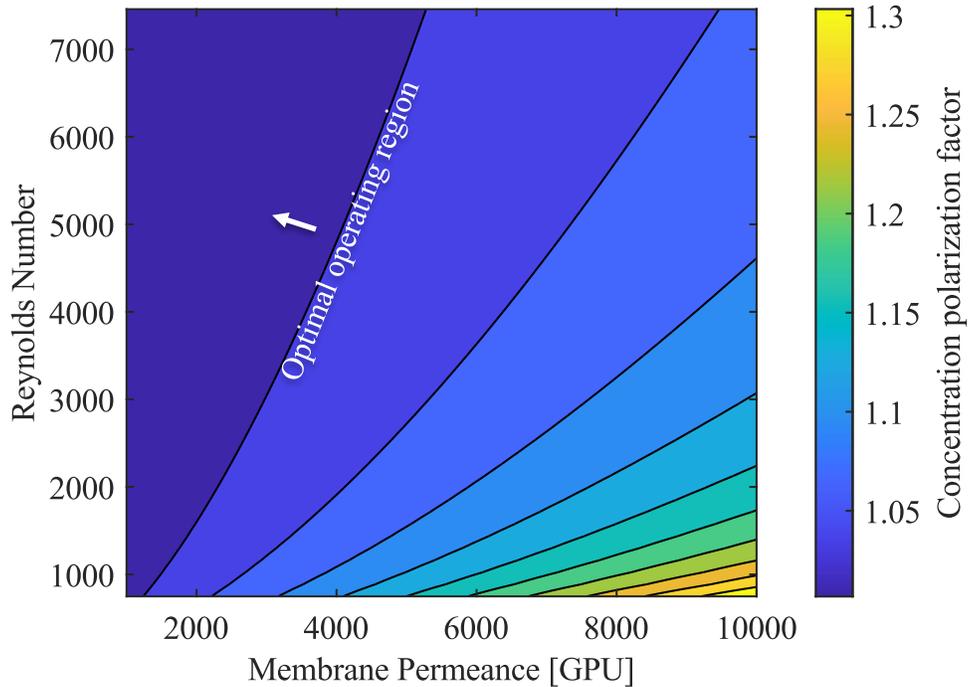
Figure 16: Impact of membrane permeance on humidity load to minimize normalized membrane area.

$T_{in}=27^oC$, $RH_{in}=70\%$, $T_{coil}=10^oC$ with L x H x W as 0.8 m x 0.006 m x 0.3m, $N_{coils}=8$, $v_{os}=$ 0.006m and $h_{os}=0.08$ m. Operating the membrane heat exchanger in turbulence regime helps avoid concentration polarization (top left region).

2.6.8   Effect of Reynolds number on number of cooling coils

The sensible load requirement of membrane heat exchanger decides the number of coils in the channel. The number of cooling coils and its dependence on the Reynolds number and temperature change is shown in figure 12. To achieve a cooler air in extremely hot climate (at temperature difference of 20^OC), large number of coils (20) are required when the flow is laminar. Increasing the Reynolds number from laminar to transition regime reduces the number of coils required by 55% and increasing the Reynolds number from laminar to turbulent region reduces the number of coils required by ~78%. The number of coils is also dependent on the membrane permeance and the humidity load which affects the membrane's ability to dehumidify the air before condensation. Hence, changing the membrane permeance and humidity load will also change the number of coils required by changing the horizontal coil spacing.

30
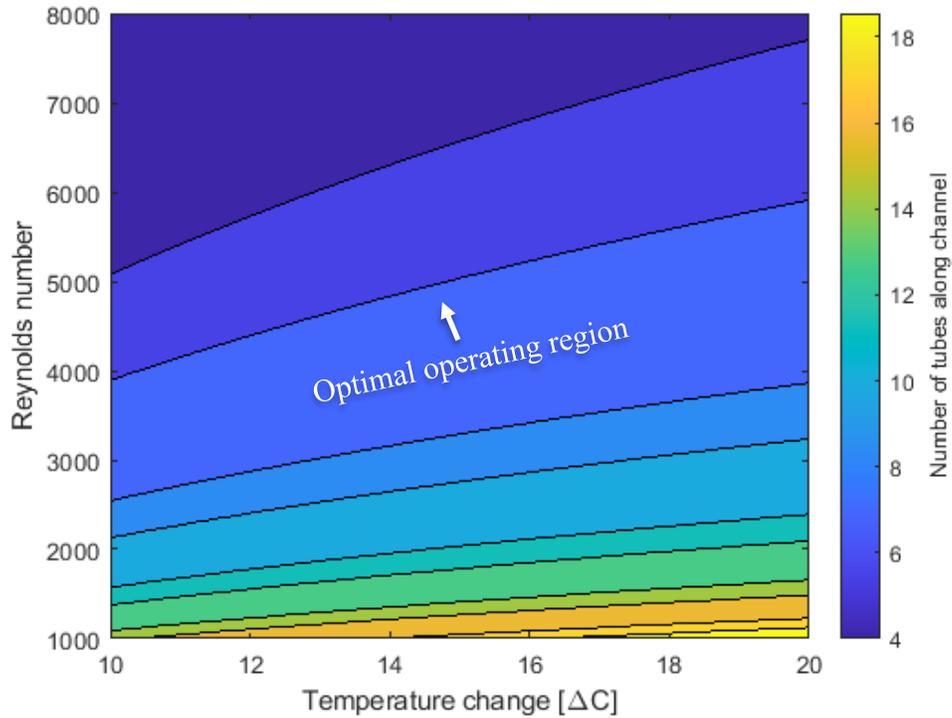
Figure 17: Number of tubes required for cooling of air with respect to Reynolds number.

T_{in}= 27°C, RH$_{in}$= 70%, with H x W as 0.006 m x 1m, v_{os}= 0.006m. B=5000 GPU. Transitioning from laminar to turbulent flow causes substantial decrease in required tubes which is then weakly improved by further Re increases

2.6.9 Membrane permeance effect on horizontal coil spacing

The membrane permeance has a strong influence on the horizontal coil spacing required to dehumidify the air before it condenses. Modifying these values will also change the horizontal coil spacing required for the coils to avoid condensation.   The ΔT in y axis represents difference between dew point temperature for given inlet conditions and different coil temperatures. Maintaining the coil temperature farther below from the dew point temperature for a lower membrane permeance requires the coil to be placed father apart from the feed of channel inlet as the mass flux of water through the membrane is greatly inhibited by its permeance value. Increasing membrane permeance from 2000 GPU to 6000 GPU for the same temperature difference minimized the coil spacing by 60% as expected. A similar explanation can be given for maintaining coil temperature closer to dew point for different membrane permeance values.
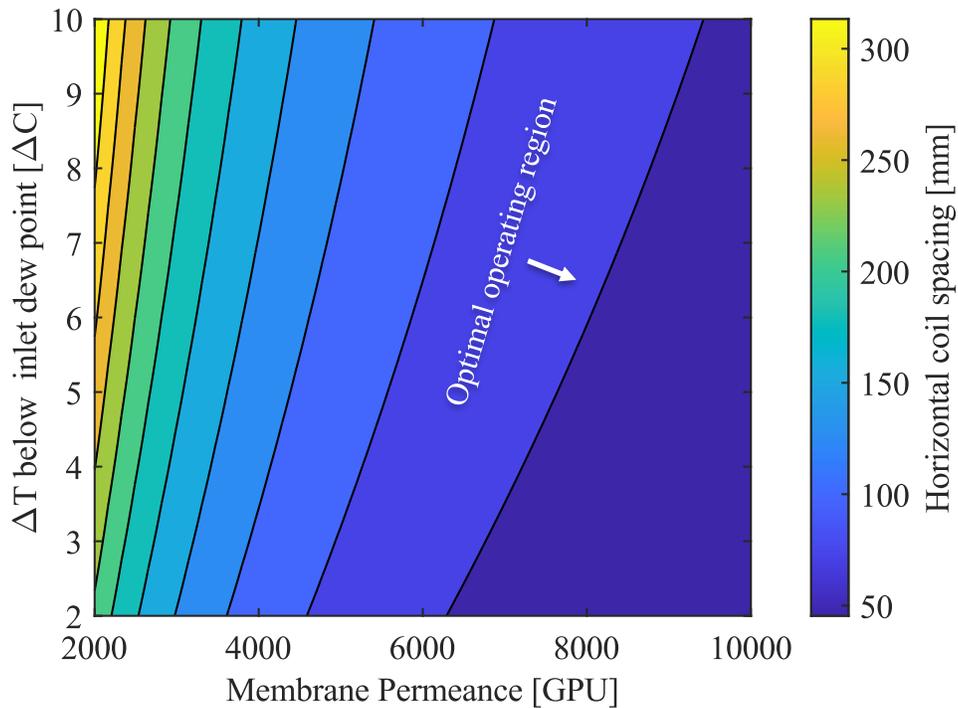
Figure 18: Horizontal coil spacing optimization to avoid condensation.

T_{in}=27°C RH_{in}= 70%, with L x H x W as 0.8 m x 0.006 m x 1m, v_{os}= 0.006m, Re = 4000. The number of cooling coils were decided based on horizontal coil spacing and target temperature to be achieved at the channel outlet.

2.7 Conclusions

A CFD model was built to develop contour plots which could be used to understand the tradeoffs between different design parameters of membrane heat exchanger. The important conclusions from the graph are given below

- The membrane area required for dehumidification and effects of concentration polarization minimizes with a turbulent Reynolds number and an optimal channel length. However, operating at high turbulence regimes can also result in higher pressure drops

- There exists an optimal coil diameter to channel height ratio that minimizes the channel pressure drop.

- A variable horizontal coil spacing is required to avoid condensation along channel length while having the optimal membrane area to dehumidify the air

- Operating the channel in turbulence regime helps to minimize the membrane area for dehumidification and effect of concentration polarization.

32

- An optimal membrane permeance value was found to be in the range of 5000-6000 GPU. Increasing the membrane permeance further does not yield major benefits
- Operating the membrane heat exchanger with a higher membrane permeance, large channel length and a high turbulent Reynolds number does not yield benefits
- The study shows that it is optimal to operate the membrane heat exchanger in a slightly turbulent regime since operating in high turbulent regimes does not yield major benefits
- The area required for the mass transfer in a membrane heat exchanger is 16 times more than the area required for heat transfer based on the current CFD study results.

2.8   References

[1]   EIA. Annual Energy Outlook. Table: Commercial Sector Key Indicators and Consumption. Reference   Case.   Accessed   August   2017.   Available   at: https://www.eia.gov/outlooks/aeo/data/browser/#/?id=5-AEO2017&cases=ref2017&sourcekey=0

[2]   William Goetzler, Richard Shandross, Jim Young, Oxana Petritchenko, Decker Ringo, Sam McClive,2017, Energy Savings Potential and RD&D Opportunities for Commercial Building HVAC Systems, Office of Energy Efficiency & Renewable Energy, U.S Department of Energy, United States

[3]   L.Z. Zhang, Energy performance of independent air dehumidification systems with energy recovery measures, Energy, vol 31,pp 1228-1242,2006.

[4]   Kevin K.W. Wan, Danny H.W. Li, Dalong Liu, Joseph C. Lam, Future trends of building heating and cooling loads and energy consumption in different climates, Building and Environment, vol 46, pp 223-234,2011.

[5]   Brent D. Yacobucci, Energy Policy: 114th Congress Issues, Congressional Research Services, Center for Homeland Defense and Security,Canada September 30, 2016

[6]   US Department of Energy, An Assessment of Energy Technologies and Research Opportunities, Chapter 5, Increasing Efficiency of Building Systems and Technologies, September 2015

[7]   Goetzler W, Zogg R, Young J, Johnson C. Energy savings potential and RD&D opportunities for non-vapor-compression HVAC technologies, Office of Energy Efficiency & Renewable Energy, U.S Department of Energy, United States, 2014.

[8]   Shengwei Wang, Xinhua Xu, Optimal and robust control of outdoor ventilation airfow rate for improving energy efficiency and IAQ,Building and Environment, vol 39, pp 763-773,2004

[9]   Vahid Vakiloroaya, Bijan Samali, Ahmad Fakhar, Kambiz Pishghadam, A review of different strategies for HVAC energy saving, Energy Conversion and Management, vol 77, pp 738-754, 2014

[10]   Yu Huang, Jian-lei Niu, A review of the advance of HVAC technologies as witnessed in ENBpublications in the period from 1987 to 2014, Energy and Buildings, vol 130, pp 33-45, 2016

[11]   Wei Liang, Rebecca Quinte, Xiaobao Jia, Jian-Qiao Sun, MPC control for improving energy efficiency of a building air handler for multi-zone VAVs, Building and Environment, vol 92, pp 256-268, 2015

[12]   Xinqiao Jin , Zhimin Du, Xiaokun Xiao, Energy evaluation of optimal control strategies for central VWV chiller systems, Applied Thermal Engineering, vol 27, pp 934-941, 2007

[13]   Goetzler W, Zogg R, Young J, Johnson C. Alternatives to vapor-compression HVAC technology. ASHRAE Journal, vol 56,pp 12-14,16,18,20-23, 2014.

[14]   Kambiz Tahvildari, Seyed Mohammad Reza Razavi, Hamed Tavakoli, Ashkan Mashayekhi, Reza Gol Mohammadzadeh, Modeling and simulation of membrane separation process using computational fluid dynamics, Arabian Journal of Chemistry, vol 9, pp 72-78, 2016.

[15]   M Rezaei, A Alsaati, DM Warsinger, F Hell, WM Samhaber, Long-Running Comparison of Feed-Water Scaling in Membrane Distillation, Membranes   10 (8), 173 2020

[16]   F. Du, D. M. Warsinger, T. Urmi, G. P. Thiel, A. Kumar, and J. H. Lienhard, "Sodium hydroxide production from seawater desalination brine: process design and energy efficiency," Environmental science & technology,Vol 10, 2018

[17]   J. Woods and E. Kozubal, Heat transfer and pressure drop in spacer-filled channels for membrane energy recovery ventilators, Applied Thermal Engineering, vol. 50, no. 1. pp. 868–876, 2013.

[18]   P. D. Armatis and B. M. Fronk, Evaluation of governing heat and mass transfer resistance in membrane-based energy recovery ventilators with internal support structures, Science Technolgy For Built Environment, vol. 23, no. 6, pp. 912–922, 2017.

[19]   M. A. Gjennestad, E. Aursand, E. Magnanelli, and J. Pharoah, Performance analysis of heat and energy recovery ventilators using exergy analysis and nonequilibrium thermodynamics, Energy and Buildings, vol. 170. pp. 195–205, 2018.

[20]   Jason Woods, Membrane processes for heating, ventilation and air conditioning, Renewable and Sustainable Energy Reviews, vol 33, pp 290-304,2014

[21]   L.Z.Zhang, X.R.Zhang, Q.Z.Miao, L.X.Pei, Selective permeation of moisture and VOCs through polymer membranes used in total heat exchangers for indoor air ventilation. Indoor Air ,vol 22, pp 321–30, 2012

[22]   Lowenstein, A. Slayzak, S. Ryan J. Pesaran, A. Advanced commercial liquid- desiccant technology development study. National Renewable Energy Laboratory. NREL/TP-550-24688; 1998.

[23]   Pietro Mazzei, Francesco Minichiello, Daniele Palma, HVAC dehumidification systems for thermal comfort:A critical review, Applied Thermal Engineering,vol 25, pp 677-707, 2005.

[24]   Xia Fang, Jon Winkler & Dane Christensen Using Energy Plus to perform dehumidification analysis on Building America homes, HVAC&R Research, vol 17, pp 268-283, 2011.

[25]   Omar Labban, Tianyi Chen, Ahmed F. Ghoniem, John H. Lienhard, Leslie K. Norford, Next-generation HVAC: Prospects for and limitations of desiccant and membrane-based dehumidification and cooling, Applied Energy, vol 200, pp 330 – 346, 2017

[26]   Vallieres C, FavreE, Vacuum versus sweeping gas operation for binary mixtures separation by dense membrane processes, Journal of Membrane Science, vol 244,pp 17–23, 2004.

[27]   Hanlon P,editor. Compressor hand book, McGraw-Hill,NewYork , 2001.

[28]   Guozhao, Guoxiong Wang, Kamel Hooman, Suresh Bhatia, João C. Diniz da Costa, Computational fluid dynamics applied to high temperature hydrogen separation membranes, Front. Chem. Sci. Eng, vol 6, pp 2-12,2012.

[29]   M. Shakaib, S.M.F. Hasani, M. Mahmood, CFD modeling for flow and mass transfer in spacer-obstructed membrane feed channels, Journal of Membrane Science,vol 326,pp 270-284,2009.

[30] T. D. Bui, Y. Wong K. Thu S.J. Oh M. Kum Ja K.C. Ng I. Raisul K.J. Chua, Effect of hygroscopic materials on water vapor permeation and dehumidification performance of poly(vinyl alcohol) membranes, Journal of Applied Polymer Science, vol. 134, pp. 1–9, 2017.

[31] R. Ghidossi, D. Veyret, P. Moulin, Computational fluid dynamics applied to membranes: State of the art and opportunities, Chemical Engineering and Processing, vol 45, pp 437-454,2016.

[32] D. B. Lu, D. M. Warsinger, Energy savings of retrofitting residential buildings with variable air volume systems across different climates, Journal of Building Engineering, vol 30, pp 101223, 2020.

[34] A. Fix, J. E. Braun, D. M. Warsinger, Vapor-Selective nanostructured membrane heat exchangers for cooling and dehumidification, U.S. Provisional application. PRF number 2020-WARS-68838, February 2020.

[34] Andrew J Fix, James E Braun,David M Warsinger, Vapor Selective membrane heat exchanger   for high efficiency outdoor air treatment, Applied Energy (in review)

[35] D. E. Claridge and C. Culp, Systems and methods for air dehumidification and cooling with membrane vapor rejection, US 8,500,848 B2, 2013.

[36] T. Chen and L. K. Norford, "Energy Performance of Next-Generation Dedicated Outdoor Air-Cooling Systems in Low-Energy Building Operations," Energy Buildings, vol. 209, 2020.

[37]   Nam Kho, Huynha, Hua Lib, Yeng Chai Soh, Wenjian Cai, Performance characterization of the membrane-based energy recovery system, International Conference on Materials for Advanced Technologies, Procedia Engineering, vol214, pp 50-58,2017.

[38]   Khadije El Kadi1, Isam Janajreh, Raed Hashaikeh, Numerical simulation and evaluation of spacer-filled direct contact membrane distillation module,Applied Water Science, vol 10, pp 1-17,2020.

[39] Rebecca Schwantes, Jakob Seger, Lorenz Bauer, Daniel Winter, Tobias Hogen, Joachim Koschikowski, Sven-Uwe Geißen, Characterization and assessment of a novel plate and frame MD module for single pass waste water concentration–feed gap air gap membrane distillation, Membranes, vol 9,pp 1-28,2019.

[40]   Jincheng Lou, Johan Vanneste, Steven C. DeCaluwe, Tzahi Y. Cath, Nils Tilton, Computational fluid dynamics simulations of polarization phenomena in direct contact membrane distillation, Journal of Membrane Science, vol 591, pp 1- 18, 2019.

[41]   G. Zschaeck, T. Frank, A.D. Burn, CFD modelling and validation of wall condensation in the presence ofnon-condensable gases, Nuclear Engineering and Design, vol 279, pp 137-146, 2014.

[42]   D. Bergmair, S.J. Metz, H.C. de Lange, A.A. van Steenhoven, System analysis of membrane facilitated water generation from air humidity, Desalination, vol 339, pp 26 -33

[43]   D.Bergmair, S.J. Metz, H.C. de Lange, A.A. van Steenhoven , A low pressure recirculated sweep stream for energy efficient membrane facilitated humidity harvesting, Separation and Purification Technology,vol 150, pp 112-118,2015.

[44]   S. J. Metz, W. J. C. Van De Ven, J. Potreck, M. H. V. Mulder, and M. Wessling, Transport of water vapor and inert gas mixtures through highly selective and highly permeable polymer membranes, Journal of Membrane Sciences, vol. 251, no. 1–2, pp. 29–41, Apr. 2005

[45]   T. D. Bui, A. Nida, K. C. Ng, and K. J. Chua, Water vapor permeation and dehumidification performance of poly(vinyl alcohol)/lithium chloride composite membranes, Journal of Membrane Science, vol. 498, pp. 254–262, 2016.

[46]   F. H. Akhtar, Hakkim Vovusha, Luis Francisco Villalobos, Rahul Shevate, Highways for water molecules: Interplay between nanostructure and water vapor transport in block c opolymer membranes, Journal of Membrane Science, vol. 572. pp. 641–649, 2019.

[47]   Y. Shin, Birgit Schwenzer; Bojana Ginovska; David W. Gotthold, Graphene oxide membranes with high permeability and selectivity for dehumidification of air, Carbon, vol. 106, pp. 164–170, 2016.

[48]   F. H. Akhtar, M. Kumar, and K. V. Peinemann, Pebax®1657/Graphene oxide composite membranes for improved water vapor separation, Journal of Membrane Science, vol. 525, pp. 187–194, 2017.

[49]   H. Sijbesma, K. Nymeijer, R. van Marwijk, R. Heijboer, J. Potreck, and M. Wessling, Flue gas dehydration using polymer membranes, Journal of Membrane Science, vol. 313, pp. 263–276, 2008.

[50] T. Puspasari, F. H. Akhtar, W. Ogieglo, O. Alharbi, and K. V. Peinemann, High dehumidification performance of amorphous cellulose composite membranes prepared from trimethylsilyl cellulose, Journal of Material Chemistry A, vol. 6, pp. 9271–9279, 2018.

[51] Jens Potreck, Kitty Nijmeijer, Thomas Kosinski, Matthias Wessling, Mixed water vapor/gas transport through the rubbery polymer PEBAX® 1074, Journal of Membrane Science, vol 338, pp 11-16,2009.

[52] S.J. Metz, W.J.C. van de Ven, J. Potreck, M.H.V. Mulder, M. Wessling, Transport of water vapor and inert gas mixtures through highly selective and highly permeable polymer membranes, Journal of Membrane Science, vol 251, pp 29-41,2005.

[53] Muhammad Irshad Baig, Pravin G. Ingole, Jae-deok Jeon, Seong Uk Hong, Won Kil Choi, Boyun Jang, Hyung Keun Lee, Water vapor selective thin film nanocomposite membranes prepared by functionalized silicon nanoparticles, Desalination, vol 451, pp 59-71, 2019.

[54] W.A. Khan, J.R. Culham , M.M. Yovanovich, Convection heat transfer from tube banks in crossflow: Analytical approach, International Journal of Heat and Mass Transfer,vol 49, pp 4831-pp5838,2006

[55] A.Žukauskas, Heat Transfer from Tubes in Crossflow,Advances in Heat Transfer,vol 8,pp 3-160,1972.

[56] International Energy Agency, The future of cooling, 2020, <https://www.iea.org/reports/the-future-of-cooling>

4. RESEARCH CONTRIBUTION AND FUTURE WORK

The work in this study aims to reduce the energy consumption and environmental impact caused by use of refrigerants in vapor compression cooling technology through the use of alternative membrane-based technologies. This study consists of two main components: CFD modeling and design of an improved membrane heat exchanger system and developing contour plots to understand the system performance under different operating conditions.

Two important contributions from this study are: The membrane heat exchanger is more limited by the membrane area than the heat transfer area. This means that more membrane area is required to dehumidify the air before it condenses in the channel. Operating the membrane heat exchanger in very high turbulence regime does not yield benefits and results in high pressure drops. Hence it is advisable to operate in a slightly turbulence regime.

The next step in the project will be building an experimental lab type prototype of the membrane heat exchanger along with necessary instrumentation required for recording the important design variables like the temperature, relative humidity. This will help understand the membrane heat exchanger performance in real time environment. The current CFD model needs to be modified further to account match with the results of the prototype which will help the model account for some of the real time operating parameters such as additional heating caused by fans and friction. This model can then be further used to study and evaluate different optimized configurations of the membrane heat exchanger in real time

APPENDIX A. MESHING AND CFD MODEL DETAILS

The following figure shows the meshing details of 2D CAD model used in CFD model for the study. The following mesh is the initial mesh generated of the base model which is used to obtain the optimized mesh size using mesh independence study.
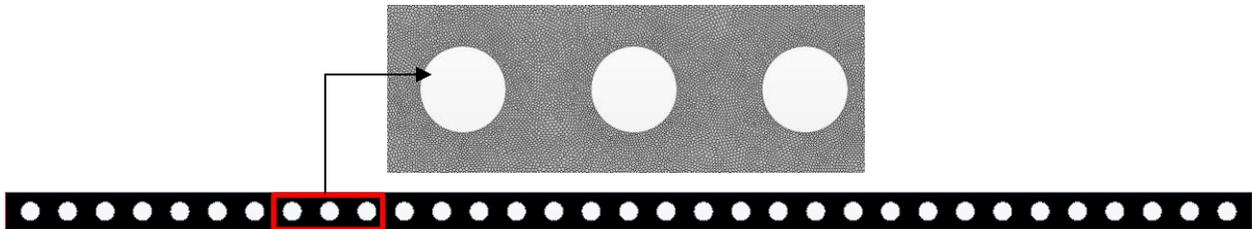

Figure S 1: Meshing of base model used in the study. L x W x H= 0.2 m x 0.006 m x 1 m

Mesh independence study results are shown in following figure
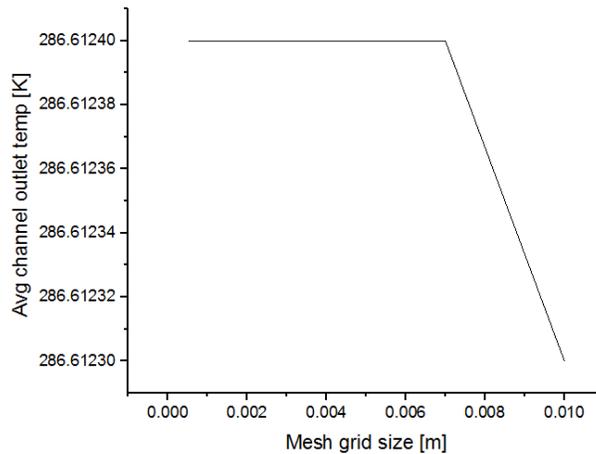
Figure S 2: Meshing independence study. L x W x H= 0.2 m x 0.006 m x 1 m.

The following figure shows convection coefficient and pressure contour results obtained from CFD study for the base model which is used as a validation against the analytical model
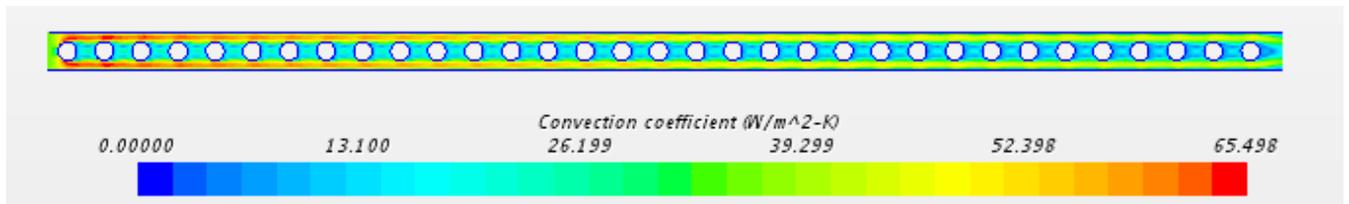
Figure S 3: Heat transfer coefficient results from CFD. L x W x H= 0.2 m x 0.006 m x 1 m, N_{coils} = 33, $d_{cooling\ coils}$ =3mm, v_{in}=1m/s,T_{in}=27°C, RH_{in}=70%, T_{coil}=10°C, B=5000 GPU.

Figure S 4: Pressure drop results from CFD. L x W x H= 0.2 m x 0.006 m x 1 m, N_{coils} = 33, $d_{cooling\ coils}$ =3mm, v_{in}=1m/s,T_{in}=27°C, RH_{in}=70%, T_{coil}=10°C, B=5000 GPU.

APPENDIX B. ANALYTICAL MODEL VALIDATION

The following figure shows the configuration of in line tube bank for which analytical model is used as a reference to validate CFD results.
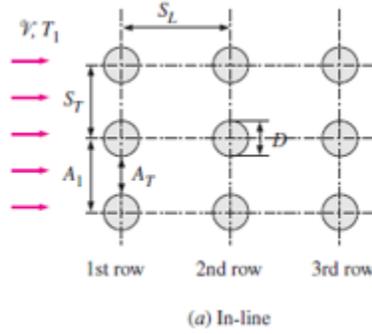

(a) In-line

Figure S 5: Geometry of analytical model used for validation of CFD model used in the study

The temperature drop of the fluid flowing across a in line cylinder tube bank is calculated using the equation

$$T_E = T_s - [\ T_s - \ T_i]e^{\frac{h\,A_s}{m\,C_p}} \tag{S2}$$

T_E is the exit temperature after each column of tube bank, T_s is the surface temperature of tube banks, T_i is the inlet temperature of fluid prior to entering the tube bank, m is the mass flow rate of fluid through tube bank, C_p is the specific heat of fluid , A_s is the surface area of all tubes in the tube bank, h is the convection coefficient of tube bank obtained from Nusselt number correlation for inline tube bank depending on Reynolds number given by

$$Nu = 0.27Re_D^{0.63}Pr^{0.36}\left(\frac{Pr}{Pr_s}\right)^{0.25} \quad 1000 \leq Re \leq 2 \times 10^5 \tag{S3}$$

Where Re_D is the Reynolds number at the hydraulic diameter of the channel, Pr is Prandtl number at average temperature of fluid given by average of inlet and outlet temperatures of tube bank, Pr_s is the Prandtl number at surface temperature of the tube bank. The convection coefficient obtained

from analytical correlation is $56W/m^2K$. The pressure drop of fluid flowing across tube bank is calculated using the correlation

$$\Delta P = N_L f \chi \frac{\rho V_{max}^2}{2} \qquad (S4)$$

where V_{max} is the maximum velocity of fluid in tube bank given by

$$V_{max} = \frac{S_T}{S_T - D} \qquad (S5)$$

where S_T is the transverse pitch which is the vertical coil spacing and D is the diameter of the cooling tube, f is the friction factor obtained from Reynolds number Vs friction factor graph for inline tube banks and χ is correction factor to account for deviation of tube arrangement in the channel from a square configuration. To calculate the temperature, drop across the tube, the number of tubes is considered as length in x direction. For example: A single tube refers to a distance of 6mm along the channel.

APPENDIX C. CFD MODEL MASS TRANSFER QUALITATIVE VALIDATION

The salt concentration results on the membrane surface reported from the CFD study of a flat plate DCMD process (concentration of salts at membrane surface) along the dimensionless channel length as a function of the dimensionless channel aspect ratio with working fluid as water vapor/salt as the working fluid is shown below. The solid line represents the membrane surface concentration results from CFD and the dotted line represents the membrane surface concentration determined using Sherwood correlations. The study models the mass transfer across the membrane as a linear function of transmembrane pressures which are an exponential function of the membrane temperature.
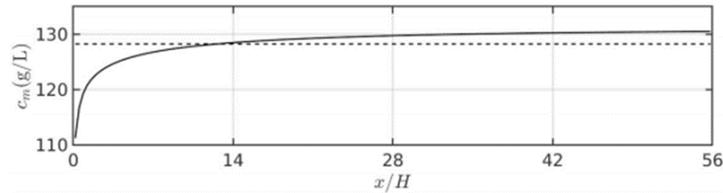

Figure S 6: Membrane surface salt concentration variation along channel length from CFD and sherwood number correlations[40]. L=17.78 cm, H=3.175 mm T_{in}=60°C , C_{in}=100g/L, v_{in} = 0.124m/s, B=1.8676×10−6 kg/m^2 s Pa.

The trends of this study match well with the trends of water vapor concentration at membrane surface reported in the current study
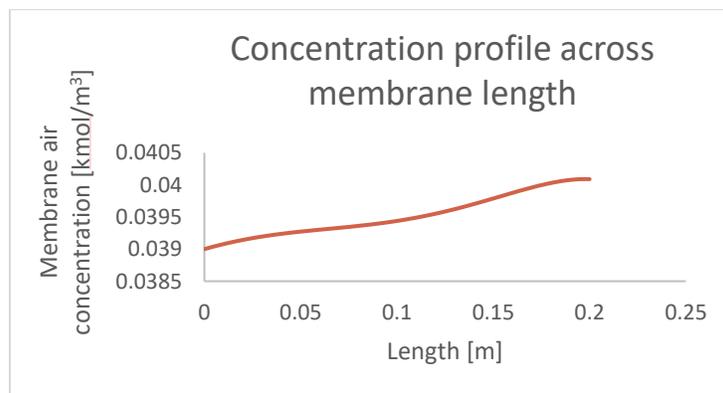

Figure S 7: Concentration profile of water vapor at membrane surface from CFD. L x W x H= 0.2 m x 0.006 m x 1 m v_{in}=1m/s,T_{in}=27°C, RH_{in}=70%, T_{coil}=10°C, B=5000 GPU.

The reason behind the curvature of concentration in the current study is due to presence of cooling coils integrated with the channel which causes slight mixing of water vapor/air mixture. There is also a slope difference because of difference in membrane permeance values used is the study. Additionally, in the reference study, the vapor pressure at the membrane surface is modelled as a exponential function of membrane surface temperature while in the current study, the vapor pressure is modelled as function of local membrane concertation and vapor pressure values

The concentration trends of the salts from CFD study reported by the validation study are shown below
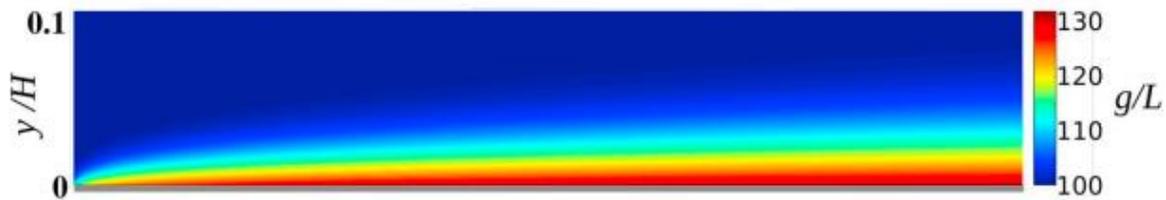
Figure S 8: Membrane surface salt concentration contours from CFD along channel length[40]. L=17.78 cm, H=3.175 mm T_{in}=60°C , C_{in}=100g/L, v_{in} = 0.124m/s, B=1.8676×10−6 kg/m^2 s Pa.

Figure S 9: Water vapor contour results from CFD study. L x W x H= 0.2 m x 0.006 m x 1 m. N_{coils} = 33, $d_{cooling\ coils}$ =3mm, v_{in}=1m/s,T_{in}=27°C, RH_{in}=70%, T_{coil}=10°C, B=5000 GPU.

The contour plots from the results section are obtained with matlab after performing the necessary simulations of 50 data points for the required conditions with CFD. The contour plots on matlab can be obtained using the following commands

```
contourf(X,Y,Z,N);
xlabel('X axis title');
ylabel('Y axis title');
ylabel(h,'Z axis title [units]');
```

Where X and Y are the independent variables along the X and Y axis, Z is the dependent variable on the contour scale which is a function of both X and Y variables, N refers to the number of contour levels required in the graph and is taken as 10 for the current case

Preliminary results for vacuum assisted air gap system are shown below

3mm

P_{in} =31500 Pa

T_{in} = 343 K

Vapor

P_{abs} =10000Pa

1000mm

T = 320 K

m_{sink}
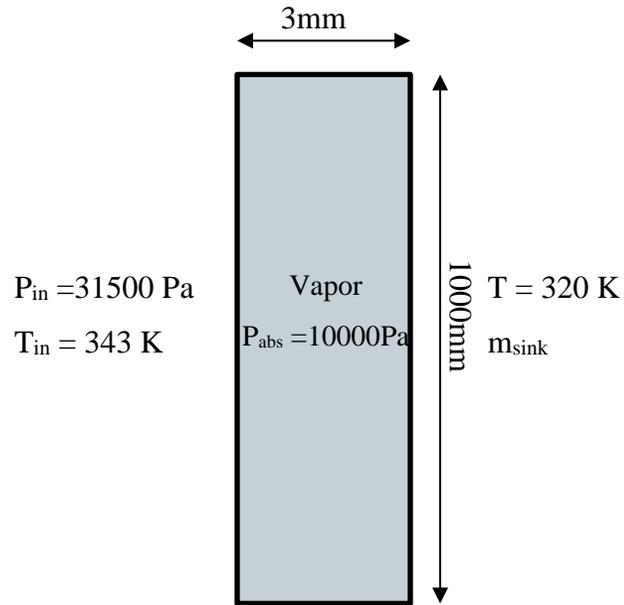
Figure S10a: Vacuum assisted air gap membrane distillation setup (VA-AGMD)with boundary conditions

Temperature (K)
343.69
338.95
334.21
329.48
324.74
320.00

Velocity: Magnitude (m/s)
0.55632
0.44505
0.33379
0.22253
0.11126
0.00000
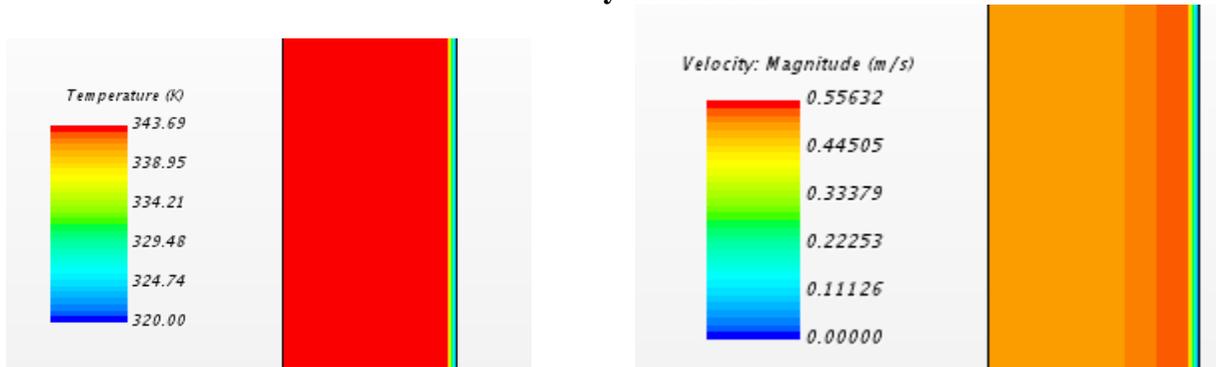
Figure S10b: Temperature results on left and velocity results on right for AGMD setup